

Distance-Based Kinematics of the Five-Oblique-Axis Thumb Model with Intersecting Axes at the Metacarpophalangeal Joint

Nicolas Rojas, *Member, IEEE* and Aaron M. Dollar, *Senior Member, IEEE*

Abstract—This paper proposes a novel and simple method to compute all possible solutions of the inverse kinematics problem of the five-oblique-axis thumb model with intersecting axes at the metacarpophalangeal joint. This thumb model is one of the suggested results by a magnetic-resonance-imaging-based study that, in contrast to those based on cadaver fingers or on the tracking of the surface of the fingers, takes into account muscle and ligament behaviors and avoids inaccuracies resulting from the movement of the skin with respect to the bones. The proposed distance-based inverse kinematics method eliminates the use of arbitrary reference frames as is usually required by standard approaches; this is relevant because the numerical conditioning of the resulting system of equations with such traditional approaches depends on the selected reference frames. Moreover, contrary to other parametrizations (e.g., Denavit-Hartenberg parameters), the suggested distance-based parameters for the thumb have a natural, human-understandable geometric meaning that makes them easier to be determined from any posture. These characteristics make the proposed approach of interest for those working in, for instance, measuring and modeling the movement of the human hand, developing rehabilitation devices such as orthoses and prostheses, or designing anthropomorphic robotic hands.

I. INTRODUCTION

The relevance of the human thumb in our daily activities related to manipulation is evident. The thumb plays a fundamental role whenever we make physical changes to the environment, from those resulting from precise pinches and powerful grasps to those performed by the fine repositioning of objects. Because of this importance, realistic biomechanical models of the thumb are essential to understand the functional sequels of orthopedic and neurological diseases and their corresponding treatments and (robotic) rehabilitation procedures [1]. An indispensable step to this end is to develop an accurate kinematic model of the thumb's joints, since the calculations of muscle and external forces depend on its kinematic structure [2]. In fact, it has been shown that simplistic kinematic descriptions of the thumb cannot predict lifelike fingertip forces [3].

However, the thumb has complex kinematics that have been challenging to model using traditional approaches. The human thumb has three joints: 1) the carpometacarpal (CMC) joint between the carpal (trapezium) and metacarpal bones, 2) the metacarpophalangeal (MCP) joint between the metacarpals and proximal phalanges, and 3) the interphalangeal (IP) joint between proximal and distal phalanges

N. Rojas is with the Dyson School of Design Engineering, Imperial College London, London SW7 1NA, UK. n.rojas@imperial.ac.uk
A. M. Dollar is with the Department of Mechanical Engineering and Materials Science, Yale University, New Haven, CT USA. aaron.dollar@yale.edu.

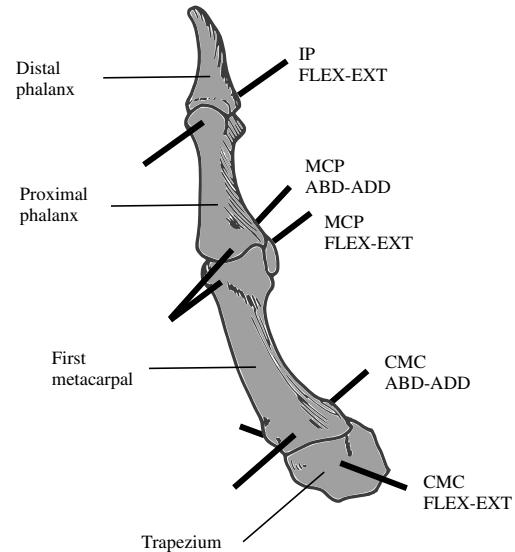


Fig. 1. Kinematic model of the thumb herein analyzed. This model is composed of five-oblique revolute axes: two non-parallel, non-orthogonal, non-intersecting axes of rotation at the carpometacarpal (CMC) joint, one for flexion-extension (CMC FLEX-EXT) and one for abduction-adduction (CMC ABD-ADD); two non-parallel, non-orthogonal, intersecting axes of rotation at the metacarpophalangeal (MCP) joint, one for flexion-extension (MCP FLEX-EXT) and one for abduction-adduction (MCP ABD-ADD); and one axis of rotation at the interphalangeal (IP) joint for flexion-extension (IP FLEX-EXT).

(Fig. 1). While there has been substantial research on the structure of the thumb, it seems that the consensus of the research community is that the thumb model proposed in [2], obtained using a cadaver finger, is a realistic representation of the mechanical degrees of freedom. This model consists of five revolute axes: two non-parallel, non-orthogonal, non-intersecting axes of rotation at the CMC joint, one for flexion-extension (CMC FLEX-EXT) and one for abduction-adduction (CMC ABD-ADD); two non-parallel, non-orthogonal, non-intersecting axes of rotation at the MCP joint, one for flexion-extension (MCP FLEX-EXT) and one for abduction-adduction (MCP ABD-ADD); and one axis of rotation at the IP joint for flexion-extension (IP FLEX-EXT).

Of particular interest to kinematics modeling, the non-intersecting MCP axes makes the problem challenging, especially due to anatomical variability. For example, using results from mechanical axis finder studies, it was found in [1] that the order of the MCP joint axes, which are in general modeled with the flexion-extension axis distal to the adduction-abduction axis, can change. Moreover, studies that

compare whether a universal joint model (*i.e.*, intersecting and orthogonal axes) is more accurate than a non-orthogonal, non-intersecting model for the MCP joint of the thumb have not yet been performed [4]. Indeed, there is no a general agreement about which simplifications of the model proposed in [2] are acceptable, or how it can be improved.

The proposed approach relies on the assumption that the MCP joint axes intersect (but can remain non-orthogonal). Axes at least sometimes intersecting is implied by [1] and there exists some empirical evidence that supports this assertion. For instance, a five-oblique-axis thumb model with intersecting MCP joint axes as shown in Fig. 1 is one of the suggested models in [5], the report of a study to determine the locations of the revolute axes of finger joints using magnetic resonance imaging images of a hand in different postures. The authors of this work argue that their technique reconstructs the active kinematics of the hand better than procedures based on hand cadavers or on tracking the surface of the fingers because it takes into account muscle synergies as well as realistic behaviors of the ligaments and avoids unknown inaccuracies resulting from the movement of the skin respect to the bones. In this paper, we propose a novel and simple method to determine all possible solutions of the inverse kinematics problem of this thumb model.

The computation of all solutions of the inverse kinematics of the five-oblique-axis thumb model with intersecting MCP axes can be done using different well-known procedures, see, for instance, [6], [7]. However, we propose a distance-based approach that eliminates the use of arbitrary reference frames as is generally required by standard methods. This is relevant because the numerical conditioning of the resulting system of equations with such traditional approaches (*i.e.*, the best possible accuracy of a solution given approximations by the computation) depends on the selected reference frames. Another advantage of our approach is that, in contrast to other parametrizations (*e.g.*, Denavit-Hartenberg parameters), the proposed distance-based parameters for the thumb have a natural, human-understandable geometric meaning that makes them easier to be determined from any posture. Thus, those working in, for instance, measuring and modeling the movement of the human hand skeleton, developing orthoses and prostheses, or designing anthropomorphic robot hands may all find these characteristics of interest.

The rest of this paper is organized as follows: section II presents the basic mathematical tools to understand the suggested approach. Section III discusses the proposed distance-based inverse kinematics method for the five-oblique-axis thumb model with intersecting axes at the MCP joint with a numerical example detailed in section IV. Finally, we conclude in section V.

II. BASICS

A. Notation

In this paper, P_i will denote a point in \mathbb{R}^3 , $\overline{P_i P_j}$ will denote the line segment between P_i and P_j , $\mathbf{p}_{i,j} = \overrightarrow{P_i P_j}$ will denote the vector from P_i to P_j , $\mathbf{p}_{i,j,k} = \mathbf{p}_{i,j} \times \mathbf{p}_{i,k}$ will denote the cross product between vectors $\mathbf{p}_{i,j}$ and $\mathbf{p}_{i,k}$,

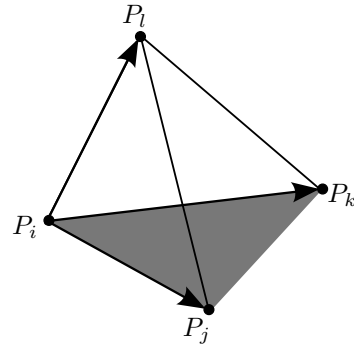


Fig. 2. A tetrahedron $\Delta_{i,j,k,l}$ with base vectors $\mathbf{p}_{i,j}$ and $\mathbf{p}_{i,k}$ and output vector $\mathbf{p}_{i,l}$ depicted. In this case, $V_{i,j,k,l} > 0$.

and $s_{i,j} = \|\mathbf{p}_{i,j}\|^2$ will denote the squared distance between P_i to P_j —squared length of $\overline{P_i P_j}$; with vector coordinates arranged as column vectors. Moreover, the non-orthonormal reference frame that in general is defined by the vectors $\mathbf{p}_{i,j}$, $\mathbf{p}_{i,k}$, and $\mathbf{p}_{i,j,k}$ will be denoted by the column vector of nine components $\mathbf{q}_{i,j,k} = (\mathbf{p}_{i,j}^T \ \mathbf{p}_{i,k}^T \ \mathbf{p}_{i,j,k}^T)^T$, the triangle defined by points P_i , P_j , and P_k will be denoted by $\Delta_{i,j,k}$, the tetrahedron defined by points P_i , P_j , P_k , and P_l will be denoted by $\Delta_{i,j,k,l}$, and the pentachoron defined by points P_i , P_j , P_k , P_l , and P_m will be denoted by $\Delta_{i,j,k,l,m}$. About a tetrahedron $\Delta_{i,j,k,l}$, according to the notation of Fig. 2, it will be said that its *base* is given by the triangle $\Delta_{i,j,k}$, its *base vectors* are $\mathbf{p}_{i,j}$ and $\mathbf{p}_{i,k}$, and its *output vector* is $\mathbf{p}_{i,l}$.

B. Cayley-Menger Determinants

An intrinsic characterization of the Euclidean metric, or Euclidean distance, in the form of a system of polynomial equations and inequalities in terms of squared interpoint distances was proposed by K. Menger in [8]; it can be expressed as

$$D(i_1, \dots, i_n; j_1, \dots, j_n) = 2 \begin{pmatrix} -1 \\ 2 \end{pmatrix}^n \begin{vmatrix} 0 & 1 & \dots & 1 \\ 1 & s_{i_1, j_1} & \dots & s_{i_1, j_n} \\ \vdots & \vdots & \ddots & \vdots \\ 1 & s_{i_n, j_1} & \dots & s_{i_n, j_n} \end{vmatrix}.$$

This determinant is known as the *Cayley-Menger bi-determinant* of the point sequences P_{i_1}, \dots, P_{i_n} , and P_{j_1}, \dots, P_{j_n} ; when the two point sequences are the same, $D(i_1, \dots, i_n; i_1, \dots, i_n)$ is abbreviated as $D(i_1, \dots, i_n)$, which is simply called the *Cayley-Menger determinant* of the involved points. Thus, for instance

$$D(i, j, k, l, m) = -\frac{1}{16} \begin{vmatrix} 0 & 1 & 1 & 1 & 1 & 1 \\ 1 & 0 & s_{i,j} & s_{i,k} & s_{i,l} & s_{i,m} \\ 1 & s_{i,j} & 0 & s_{j,k} & s_{j,l} & s_{j,m} \\ 1 & s_{i,k} & s_{j,k} & 0 & s_{k,l} & s_{k,m} \\ 1 & s_{i,l} & s_{j,l} & s_{k,l} & 0 & s_{l,m} \\ 1 & s_{i,m} & s_{j,m} & s_{k,m} & s_{l,m} & 0 \end{vmatrix}.$$

The expansion of the above equation yields a quadratic form in terms of $s_{k,l}$ and $s_{k,m}$ that can be expressed as

$$D(i, j, k, l, m) = A_{i,j,k,l,m} s_{k,l}^2 + B_{i,j,k,l,m} s_{k,l} s_{k,m} + C_{i,j,k,l,m} s_{k,m}^2 + D_{i,j,k,l,m} s_{k,l} + E_{i,j,k,l,m} s_{k,m} + F_{i,j,k,l,m}, \quad (1)$$

where

$$\begin{aligned} A_{i,j,k,l,m} &= -\frac{1}{4}D(i, j, l) \\ B_{i,j,k,l,m} &= \frac{1}{2}D(i, j, k; i, j, l) \\ C_{i,j,k,l,m} &= -\frac{1}{4}D(i, j, k) \\ D_{i,j,k,l,m} &= -D(i, j, k, l; i, j, l, m)|_{s_{k,l}=0, s_{k,m}=0} \\ E_{i,j,k,l,m} &= D(i, j, k, m; i, j, k, l)|_{s_{k,l}=0, s_{k,m}=0} \\ F_{i,j,k,l,m} &= D(i, j, k, l, m)|_{s_{k,l}=0, s_{k,m}=0}. \end{aligned}$$

The evaluation of $D(i_1, \dots, i_n)$ gives $(n-1)!$ times the squared hypervolume of the simplex spanned by the points P_{i_1}, \dots, P_{i_n} in \mathbb{R}^{n-1} [10, pp. 737-738]. Hence, we can introduce the following definitions in \mathbb{R}^3 :

- The area $A_{i,j,k}$ of the triangle $\triangle_{i,j,k}$ is $+\frac{1}{2}\sqrt{D(i, j, k)}$.
- The oriented volume $V_{i,j,k,l}$ of the tetrahedron $\triangle_{i,j,k,l}$ is $\pm\frac{1}{6}\sqrt{D(i, j, k, l)}$. It is defined as positive if $|\mathbf{p}_{i,j}, \mathbf{p}_{i,k}, \mathbf{p}_{i,l}| > 0$, and negative otherwise (see Fig. 2).
- $D(i, j, k, l, m) = 0$.

For more properties of Cayley-Menger determinants, the interested reader is referred to [9], [11].

C. Trilateration in Matrix Form

The trilateration problem consists in finding the location of a point, say P_l , whose distance to other three known points, say P_i, P_j , and P_k , is known. Given a tetrahedron $\triangle_{i,j,k,l}$, according to the notation of Fig. 2, this problem is equivalent to compute the output vector $\mathbf{p}_{i,l}$ as a function of the base vectors $\mathbf{p}_{i,j}$ and $\mathbf{p}_{i,k}$ and its squared edge distances. This computation can be expressed in matrix form as [12]

$$\mathbf{p}_{i,l} = \mathbf{W}_{i,j,k,l} \mathbf{q}_{i,j,k}, \quad (2)$$

where

$$\mathbf{W}_{i,j,k,l}^T = \frac{1}{4A_{i,j,k}^2} \begin{pmatrix} -D(i, j, k; i, k, l) \mathbf{I} \\ D(i, j, k; i, j, l) \mathbf{I} \\ 6V_{i,j,k,l} \mathbf{I} \end{pmatrix},$$

\mathbf{I} being the 3×3 identity matrix.

The vectors $\mathbf{p}_{j,l}$ and $\mathbf{p}_{k,l}$ can then be expressed as

$$\mathbf{p}_{j,l} = \mathbf{p}_{i,l} - \mathbf{p}_{i,j} = (\mathbf{W}_{i,j,k,l} - \mathbf{K}_{\text{IOO}}) \mathbf{q}_{i,j,k}, \quad (3)$$

where $\mathbf{K}_{\text{IOO}} = (\mathbf{I} \ \mathbf{O} \ \mathbf{O})$, \mathbf{O} being the 3×3 null matrix, and

$$\mathbf{p}_{k,l} = \mathbf{p}_{i,l} - \mathbf{p}_{i,k} = (\mathbf{W}_{i,j,k,l} - \mathbf{K}_{\text{OIO}}) \mathbf{q}_{i,j,k}, \quad (4)$$

with $\mathbf{K}_{\text{OIO}} = (\mathbf{O} \ \mathbf{I} \ \mathbf{O})$, respectively.

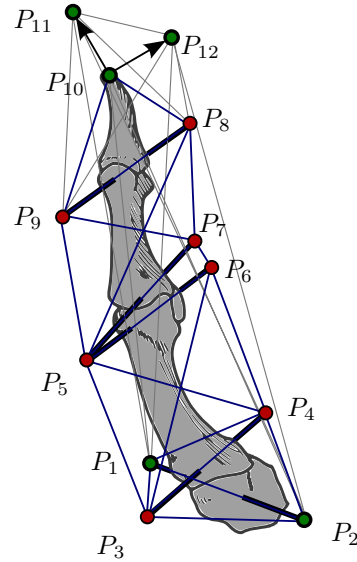


Fig. 3. The distance-based parametrization of the inverse kinematics problem of the five-oblique-axis thumb model with intersecting MCP axes generates a bar-and-joint framework composed of 12 points and 33 edges with 1 triangle, namely $\triangle_{5,6,7}$, and 3 tetrahedra, namely $\triangle_{1,2,3,4}$, $\triangle_{5,3,4,6}$, and $\triangle_{5,8,9,7}$, connecting the thumb axes, and 1 pentachoron, namely $\mathbb{P}_{8,9,10,11,12}$, connecting the IP joint flexion-extension axis to the location of the fingertip. Green circles (circles with wide border) represent points with known coordinates; red circles represent those points whose coordinates are unknown. See text for more details.

III. INVERSE KINEMATICS

The inverse kinematics problem of the five-oblique-axis thumb model with intersecting MCP axes consists in finding the possible values of the joint angles to attain a given location—position and orientation—for the fingertip relative to the location of the CMC joint flexion-extension axis.

A rigid body connecting two skew revolute axes can be modeled by taking two points on each of these axes and connecting them all with edges to form a tetrahedron [13]. Moreover, the location of the fingertip can be represented by three points, one point for position plus two points that define vectors of orientation. Thus, a distance-based parametrization of the inverse kinematics problem of the five-oblique-axis thumb model with intersecting MCP axes generates the bar-and-joint framework shown in Fig. 3. This framework is composed of 12 points, namely $P_1 \dots P_{12}$, and 33 edges, namely $\overline{P_1P_2}, \overline{P_1P_3}, \overline{P_1P_4}, \overline{P_1P_{10}}, \overline{P_1P_{11}}, \overline{P_1P_{12}}, \overline{P_2P_3}, \overline{P_2P_4}, \overline{P_2P_{10}}, \overline{P_2P_{11}}, \overline{P_2P_{12}}, \overline{P_3P_4}, \overline{P_3P_5}, \overline{P_3P_6}, \overline{P_4P_5}, \overline{P_4P_6}, \overline{P_5P_6}, \overline{P_5P_7}, \overline{P_5P_8}, \overline{P_5P_9}, \overline{P_6P_7}, \overline{P_7P_8}, \overline{P_7P_9}, \overline{P_8P_9}, \overline{P_8P_{10}}, \overline{P_8P_{11}}, \overline{P_8P_{12}}, \overline{P_9P_{10}}, \overline{P_9P_{11}}, \overline{P_9P_{12}}, \overline{P_{10}P_{11}}, \overline{P_{10}P_{12}},$ and $\overline{P_{11}P_{12}}$, with 1 triangle, namely $\triangle_{5,6,7}$, and 3 tetrahedra whose orientation is fixed, namely $\triangle_{1,2,3,4}$, $\triangle_{5,3,4,6}$, and $\triangle_{5,8,9,7}$, connecting the thumb axes, and 1 pentachoron, namely $\mathbb{P}_{8,9,10,11,12}$, connecting the IP joint flexion-extension axis to the location of the fingertip. In this pentachoron, the orientation of $\triangle_{10,11,12,8}$ and $\triangle_{10,11,12,9}$ is fixed.

In the bar-and-joint framework of Fig. 3, the length of the 33 edges as well as the coordinates of points P_1 and P_2 , corresponding to the CMC joint flexion-extension axis;

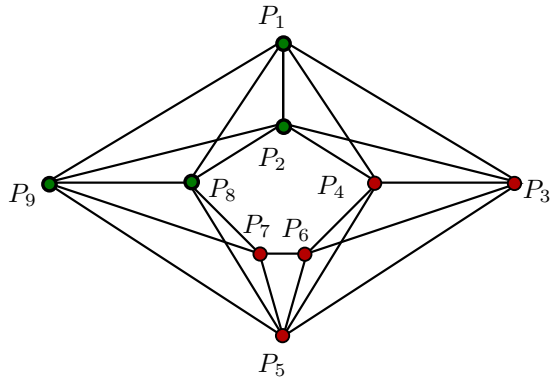


Fig. 4. After computing the location of the IP joint flexion-extension axis (points P_8 and P_9), the original bar-and-joint framework associated to the inverse kinematics problem of the five-oblique-axis thumb model with intersecting MCP axes can be replaced by a new framework composed of 9 points and 21 edges by connecting points P_1 , P_2 , P_8 , and P_9 with edges to form a tetrahedron. Green circles (circles with wide border) represent points with known coordinates; red circles represent those points whose coordinates are unknown.

points P_{10} , P_{11} , and P_{12} , corresponding to the location of the fingertip; and the orientation of tetrahedra $\triangle_{1,2,3,4}$, $\triangle_{5,3,4,6}$, and $\triangle_{5,8,9,7}$ are all known. Hence, solving the inverse kinematics problem of the five-oblique-axis thumb model with intersecting MCP axes is equivalent to computing the feasible values of points P_3 and P_4 ; P_5 , P_6 , and P_7 ; and P_8 and P_9 that define the CMC joint abduction-adduction axis, the MCP joint axes, and the IP joint flexion-extension axis, respectively. Next, we derive a simple procedure to compute these values based on the known distances between the thumb axes and the location of the fingertip.

A. The IP Joint Flexion-Extension Axis

The IP joint flexion-extension axis is defined by points P_8 and P_9 . These points can be easily computed using equation (2) from the location of the fingertip, points P_{10} , P_{11} , and P_{12} ; the length of the edges that compose the pentachoron $\mathbb{D}_{8,9,10,11,12}$; and the orientation of the tetrahedra $\triangle_{10,11,12,8}$ and $\triangle_{10,11,12,9}$ —all these values are known geometric parameters of the inverse kinematic problem. Explicitly,

$$P_8 = P_{10} + \mathbf{W}_{10,11,12,8} \mathbf{q}_{10,11,12}, \text{ and} \quad (5)$$

$$P_9 = P_{10} + \mathbf{W}_{10,11,12,9} \mathbf{q}_{10,11,12}. \quad (6)$$

This yields a single possible value for the location of the IP joint flexion-extension axis since the orientation of $\triangle_{10,11,12,8}$ and $\triangle_{10,11,12,9}$ is fixed.

B. The CMC Joint Abduction-Adduction Axis

Once the location of the IP joint flexion-extension axis is obtained, it is possible to construct a new bar-and-joint framework by connecting points P_1 , P_2 , P_8 , and P_9 with edges to form a tetrahedron. The length of the new edges $\overline{P_1P_8}$, $\overline{P_1P_9}$, $\overline{P_2P_8}$, and $\overline{P_2P_9}$ can be straightforwardly computed using the result of equations 5 and 6. The resulting framework is shown in Fig. 4.

Now, since $D(i, j, k, l, m) = 0$ in \mathbb{R}^3 , we have from the bar-and-joint framework of Fig. 4 that

$$D(8, 9, 5, 1, 2) = A1 s_{1,5}^2 + B1 s_{1,5} s_{2,5} + C1 s_{2,5}^2 + D1 s_{1,5} + E1 s_{2,5} + F1 = 0 \text{ and} \quad (7)$$

$$D(3, 4, 5, 1, 2) = A2 s_{1,5}^2 + B2 s_{1,5} s_{2,5} + C2 s_{2,5}^2 + D2 s_{1,5} + E2 s_{2,5} + F2 = 0, \quad (8)$$

where $A1 = A_{8,9,5,1,2}, \dots, F1 = F_{8,9,5,1,2}$ and $A2 = A_{3,4,5,1,2}, \dots, F2 = F_{3,4,5,1,2}$. By eliminating $s_{2,5}$ (alternatively $s_{1,5}$) from the above system of equation, we get a quartic polynomial in $s_{1,5}$ (alternatively $s_{2,5}$) that can be solved in closed-form using, for instance, Galois' solution [14] or, more conveniently, numerically using, for instance, Bairstow's method [15]. This polynomial cannot be included here for space limitation reasons, but it can be easily reproduce using a computer algebra system.

In order to compute the possible locations of the CMC joint abduction-adduction axis, that is, to determine the feasible values for P_3 and P_4 , we proceed as follows. Let t_i be the i -th real root of the quartic polynomial obtained from equations (7) and (8)—if there not exist a real root, the inverse kinematic problem has no solution. For each real root t_i —value of $s_{1,5}$ (alternatively $s_{2,5}$), we firstly compute P_5 from P_1, P_8 , and P_9 :

$$P_5 = P_1 + \mathbf{W}_{1,8,9,5} \mathbf{q}_{1,8,9}, \quad (9)$$

from which $s_{2,5}$ can be obtained. Then, points P_3 and P_4 can be computed by the next sequence of trilaterations:

$$P_3 = P_2 + (\mathbf{W}_{1,2,5,3} - \mathbf{K}_{100}) \mathbf{q}_{1,2,5} = P_1 + \mathbf{W}_{1,2,5,3} \mathbf{q}_{1,2,5}, \text{ and} \quad (10)$$

$$P_4 = P_3 + (\mathbf{W}_{1,2,3,4} - \mathbf{K}_{010}) \mathbf{q}_{1,2,3} = P_1 + \mathbf{W}_{1,2,3,4} \mathbf{q}_{1,2,3}. \quad (11)$$

Since the orientations of tetrahedra $\triangle_{1,8,9,5}$ and $\triangle_{1,2,5,3}$ are unknown and the orientation of tetrahedron $\triangle_{1,2,3,4}$ is fixed, the above procedure leads to up to four locations for P_4 . However, by geometric construction only one of them must satisfy the length of the edge $\overline{P_4P_5}$ unless tetrahedron $\triangle_{1,2,3,4}$ is flat and/or the multiplicity of t_i is greater than 1. This procedure yields a single value for P_3 , P_4 , and P_5 for each t_i .

C. The MCP Joint Axes

For each resulting location of the IP joint flexion-extension axis (points P_8 and P_9), the CMC joint abduction-adduction axis (points P_3 and P_4), and point P_5 , the feasible locations of the MCP joint axes are obtained by computing

$$P_6 = P_5 + \mathbf{W}_{5,3,4,6} \mathbf{q}_{5,3,4}, \text{ and} \quad (12)$$

$$P_7 = P_5 + \mathbf{W}_{5,8,9,7} \mathbf{q}_{5,8,9}, \quad (13)$$

and determining whether the distance between them is equivalent to the length of the edge $\overline{P_6P_7}$ —recall that the orientations of $\triangle_{5,3,4,6}$ and $\triangle_{5,8,9,7}$ are known geometric parameters; those points that satisfy this constraint are the solutions of the inverse kinematics problem along with the corresponding values for P_3 , P_4 , P_5 , P_8 , and P_9 .

TABLE I
GEOMETRIC PARAMETERS USED IN THE NUMERICAL EXAMPLE

Axes	Geometric parameters
CMC FLEX-EXT to CMC ABD-ADD	$s_{1,2} = 0.9908, s_{1,3} = 0.3566, s_{1,4} = 1.4966, s_{2,3} = 1.4566, s_{2,4} = 1.5270,$ $s_{3,4} = 1.0074, V_{1,2,3,4} < 0$
CMC ABD-ADD to MCP FLEX-EXT	$s_{3,5} = 12.0690, s_{3,6} = 15.2878, s_{4,5} = 9.8586, s_{4,6} = 11.3754, s_{5,6} = 0.9970,$ $V_{5,3,4,6} < 0$
MCP FLEX-EXT to MCP ABD-ADD	$s_{5,7} = 0.9960, s_{6,7} = 2.5098$
MCP ABD-ADD to IP FLEX-EXT	$s_{5,8} = 7.1013, s_{5,9} = 10.3013, s_{7,8} = 3.9985, s_{7,9} = 6.9185, s_{8,9} = 1.0000,$ $V_{5,8,9,7} > 0$
IP FLEX-EXT to Fingertip location	$s_{8,10} = 1.7876, s_{8,11} = 5.2676, s_{8,12} = 1.7876, s_{9,10} = 1.7876, s_{9,11} = 5.2676,$ $s_{9,12} = 3.7876, V_{10,11,12,8} > 0, V_{10,11,12,9} > 0$

IV. NUMERICAL EXAMPLE

According to the notation of Figs. 1 and 3, let us suppose that we have a five-oblique-axis thumb model with intersecting MCP axes with geometric parameters as shown in Table I. Now, let us assume that we want to compute the inverse kinematic solutions for the case in which the location of the CMC joint flexion-extension axis is given by $P_1 = (1.4400, 0.9800, 0.0000)^T$ and $P_2 = (2.4000, 0.9400, 0.2600)^T$, and the location of the fingertip is given by $P_{10} = (3.2200, -2.8100, 4.6800)^T$, $P_{11} = (3.2200, -3.8100, 4.6800)^T$, and $P_{12} = (2.22, -2.81, 4.68)^T$.

Substituting the above parameters in equations (5) and (6), we get

$$\begin{aligned} P_8 &= (2.7200, -1.5700, 4.6800)^T, \\ P_9 &= (3.7200, -1.5700, 4.6800)^T. \end{aligned} \quad (14)$$

This corresponds to the location of the IP joint flexion-extension axis. Then, $s_{1,8} = 30.0433$, $s_{1,9} = 33.6033$, $s_{2,8} = 25.9389$, and $s_{2,9} = 27.5789$, thus completing the framework of Fig. 4.

Replacing the lengths of the edges of the resulting framework from the computation of P_8 and P_9 in equations (7) and (8), we obtain

$$\begin{aligned} D(8, 9, 5, 1, 2) &= -6.4591 s_{1,5}^2 + 13.5430 s_{1,5} s_{2,5} \\ &\quad - 7.1012 s_{2,5}^2 + 5.5347 s_{1,5} - 5.6607 s_{2,5} - 2.1424 = 0, \\ D(3, 4, 5, 1, 2) &= -0.3120 s_{1,5}^2 + 0.2227 s_{1,5} s_{2,5} \\ &\quad - 0.0887 s_{2,5}^2 + 5.2067 s_{1,5} - 0.6795 s_{2,5} - 26.5069 = 0. \end{aligned}$$

The elimination of $s_{2,5}$ from the above system yields

$$\begin{aligned} 1.6393 s_{1,5}^4 - 82.4800 s_{1,5}^3 + 1514.6100 s_{1,5}^2 \\ - 12003.0912 s_{1,5} + 34717.0480. \end{aligned}$$

The real roots of this quartic polynomial are $t_1 = 9.0068$, $t_2 = 9.0245$, $t_3 = 16.0808$, and $t_4 = 16.2028$. Using each of these values in equations (9), (10), and (11), we get:

- For $t_1 = 9.0068$

$$\begin{aligned} P_3 &= (1.5246, 0.7739, -0.5540)^T, \\ P_4 &= (1.9735, -0.0830, -0.2864)^T, \\ P_5 &= (1.6200, 0.0039, 2.8322)^T. \end{aligned} \quad (15)$$

- For $t_2 = 9.0245$

$$\begin{aligned} P_3 &= (1.5420, 0.9681, -0.5883)^T, \\ P_4 &= (2.0646, 0.1112, -0.5930)^T, \\ P_5 &= (1.6200, -0.8783, 2.3534)^T. \end{aligned} \quad (16)$$

- For $t_3 = 16.0808$

$$\begin{aligned} P_3 &= (1.2300, 0.8800, 0.5500)^T, \\ P_4 &= (1.7000, 1.6500, 0.9900)^T, \\ P_5 &= (1.6200, 0.7600, 4.0000)^T. \end{aligned} \quad (17)$$

- For $t_4 = 16.2028$

$$\begin{aligned} P_3 &= (1.3009, 0.4429, 0.2208)^T, \\ P_4 &= (1.6118, 0.6241, 1.1578)^T, \\ P_5 &= (1.6200, -2.2772, 2.3581)^T. \end{aligned} \quad (18)$$

The above values correspond to the feasible locations of the CMC joint abduction-adduction axis.

Finally, using the results of equations (14), (15), (16), (17), and (18) in equations (12) and (13), we obtain

- For $t_1 = 9.0068$

$$\begin{aligned} P_6 &= (2.4696, -0.4838, 3.0255)^T, \\ P_7 &= (1.7600, -0.0416, 3.8193)^T. \end{aligned} \quad (19)$$

Squared length of $\overline{P_6 P_7} = 1.3293$.

- For $t_2 = 9.0245$

$$\begin{aligned} P_6 &= (2.5074, -1.3306, 2.4237)^T, \\ P_7 &= (1.7600, -0.5205, 3.2745)^T. \end{aligned} \quad (20)$$

Squared length of $\overline{P_6 P_7} = 1.9388$.

- For $t_3 = 16.0808$

$$\begin{aligned} P_6 &= (1.5700, 1.6900, 4.3600)^T, \\ P_7 &= (1.7600, 0.1800, 4.8000)^T. \end{aligned} \quad (21)$$

Squared length of $\overline{P_6 P_7} = 2.5098$.

- For $t_4 = 16.2028$

$$\begin{aligned} P_6 &= (1.3926, -1.9839, 3.2851)^T, \\ P_7 &= (1.7600, -1.4705, 2.9287)^T. \end{aligned} \quad (22)$$

Squared length of $\overline{P_6 P_7} = 0.5256$.

Thus, since $s_{6,7} = 2.5098$ (see Table I), there is a unique solution of the inverse kinematics problem: the values of points $P_3, P_4, P_5, P_6, P_7, P_8,$ and P_9 given by equations (14), (17), and (21).

V. CONCLUSION

The thumb model of five non-orthogonal non-intersecting revolute axes is considered by the research community as a realistic representation of the mechanical degrees of freedom in the thumb. Our approach relies on assuming that the metacarpophalangeal joint axes intersect, which is not always supported by the literature. However, there is a lack of studies that quantify how important non-intersecting MCP joint axes are, or whether a universal joint model (*i.e.*, intersecting and orthogonal axes) is more accurate than a non-orthogonal, non-intersecting model for the metacarpophalangeal joint of the thumb. Furthermore, research has shown that the order of the metacarpophalangeal joint axes, which are in general modeled with the flexion-extension axis distal to the adduction-abduction axis, can change. This absence of consensus about which simplifications of the five non-orthogonal non-intersecting axes model are acceptable, or how it can be improved, open the door to suggesting that the metacarpophalangeal joint axes may intersect in some cases and may be a perfectly acceptable simplification. Empirical evidence indeed supports this assertion; in particular, a five-oblique-axis thumb model with intersecting metacarpophalangeal joint axes is one of the suggested models by a study carried out to determine the locations of the revolute axes of finger joints using magnetic resonance imaging images of a hand in different postures. The authors of such a study argue that this method is more accurate than those based on cadaver fingers or on the tracking of the surface of the fingers.

This paper discusses a novel and simple method to determine all possible solutions of the inverse kinematics problem of the five-oblique-axis thumb model with intersecting metacarpophalangeal joint axes. The solution of this problem can be certainly obtained using different well-known procedures. However, we propose a distance-based approach that eliminates the use of arbitrary reference frames as is in general the case in standard methods. This is relevant because the numerical conditioning of the resulting system of equations with such traditional approaches (*i.e.*, the best possible accuracy of a solution given approximations by the computation) depends on the selected reference frames. Moreover, in contrast to other parametrizations (*e.g.*, Denavit-Hartenberg parameters), the suggested distance-based parameters for the thumb have a natural, human-understandable geometric meaning that makes them easier to be determined from any posture. A detailed example of how to apply the introduced approach has been presented. The solutions obtained by the proposed method can be refined by taking into account ranges of motion of the revolute axes.

REFERENCES

- [1] V. J. Santos and F. J. Valero-Cuevas, "Reported anatomical variability naturally leads to multimodal distributions of Denavit-Hartenberg parameters for the human thumb," *IEEE Transactions on Biomedical Engineering*, Vol. 53, No. 2, pp. 155 – 163, 2006
- [2] D. J. Giurintano, A. M. Hollister, W. L. Buford, D. E. Thompson, and L. M. Myers, "A virtual five-link model of the thumb," *Medical engineering & physics*, Vol. 17, No. 4, pp. 297 – 303, 1995
- [3] F. J. Valero-Cuevas, M. E. Johanson, and J. D. Towles, "Towards a realistic biomechanical model of the thumb: the choice of kinematic description may be more critical than the solution method or the variability/uncertainty of musculoskeletal parameters," *Journal of Biomechanics*, Vol. 36, No. 7, pp. 1019 – 1030, 2003
- [4] I. M. Bullock, J. Borrás, and A. M. Dollar, "Assessing assumptions in kinematic hand models: a review," in *Proceedings of the 2012 IEEE International Conference on Biomedical Robotics and Biomechatronics (BioRob)*, pp. 139 – 146, 2012
- [5] G. Stillfried, U. Hillenbrand, M. Settles, and P. van der Smagt, "MRI-based skeletal hand movement model," in *The human hand as an inspiration for robot hand development*, Springer International Publishing, pp. 49 – 75, 2014
- [6] K. K. Sugimoto and J. J. Duffy, "Analysis of five-degree-of-freedom robot arms," *ASME Journal of Mechanisms, Transmissions, and Automation in Design*, Vol. 105, No. 1, pp. 23 – 27, 1983
- [7] Y. B. Zhou and F. F. Xi, "Exact kinematic analysis of the general 5R robot," *Mechanism and Machine theory*, Vol. 33, No. 1-2, pp. 175 – 184, 1998
- [8] K. Menger, "Untersuchungen über allgemeine metrik," *Mathematische Annalen*, vol. 100, pp. 75 – 163, 1928
- [9] T. Havel, "Some examples of the use of distances as coordinates for Euclidean geometry," *Journal of Symbolic Computation*, vol. 11, pp. 579 – 593, 1991
- [10] K. Menger, "New foundation of Euclidean geometry," *American Journal of Mathematics*, vol. 53, no. 4, pp. 721 – 745, 1931
- [11] F. Thomas and L. Ros, "Revisiting trilateration for robot localization," *IEEE Transactions on Robotics*, vol. 21, no. 1, pp. 93 – 101, 2005
- [12] N. Rojas and F. Thomas, "Forward kinematics of the general triple-arm robot using a distance-based formulation," in *Proceedings of the 7th IFToMM International Workshop on Computational Kinematics*, 2017
- [13] J. Porta, L. Ros, and F. Thomas, "On the trilaterable six-degree-of-freedom parallel and serial manipulators," in *Proceedings of the 2005 IEEE International Conference on Robotics and Automation (ICRA)*, pp. 960 – 967, 2005
- [14] W. M. Faucette, "A geometric interpretation of the solution of the general quartic polynomial," *The American Mathematical Monthly*, vol. 103, no. 1, pp. 51 – 57, 1996
- [15] K. W. Brodlie, "On Bairstow's method for the solution of polynomial equations," *Mathematics of Computation*, vol. 29, no. 131, pp. 816 – 826, 1975
- [1] V. J. Santos and F. J. Valero-Cuevas, "Reported anatomical variability naturally leads to multimodal distributions of Denavit-Hartenberg